

# Improvement of biogas production from slaughterhouse wastewater using biosynthesized iron nanoparticles from water treatment sludge

Mohammad Yazdani<sup>a</sup>, Mohammadali Ebrahimi-Nik<sup>a</sup>, Ava Heidari<sup>b,\*</sup>,  
Mohammad Hossein Abbaspour-Fard<sup>a</sup>

<sup>a</sup> Department of Biosystems Engineering, Faculty of Agriculture, Ferdowsi University of Mashhad, Mashhad, Iran

<sup>b</sup> Department of Environmental Science, Faculty of Natural Resources and Environment, Ferdowsi University of Mashhad, Mashhad, Iran

## ARTICLE INFO

### Article history:

Received 24 May 2018

Received in revised form

5 September 2018

Accepted 5 December 2018

Available online 6 December 2018

### Keywords:

Drinking water treatment sludge

Iron nanoparticle

Slaughterhouse wastewater

Anaerobic digestion

## ABSTRACT

This study was conducted to examine the feasibility of recovering ferric coagulant from drinking water treatment sludge (DWTS) for green synthesis of iron nanoparticles (NPs). Black tea extract was utilized for the bio-reduction of ferric chloride. The as-synthesized product was characterized and confirmed as iron NPs, using UV–vis spectrometry, XRD, FT-IR, SEM, and EDX analyses. The synthesized NPs were sphere-like with diameter in the range of 20–40 nm. The performance of the iron NPs as micronutrients supplements in anaerobic digestion of slaughterhouse wastewater was studied at three different concentrations. The results showed that the addition of iron NPs in all concentrations improved the biogas production and shortened the lag phase. The highest biogas yield was obtained from 9 mg L<sup>-1</sup> of additive which corresponds to up to 37.6% enhancement over the control reactor. Moreover, iron NPs improved COD reduction efficiency to 42%.

© 2018 Elsevier Ltd. All rights reserved.

## 1. Introduction

Sludge produced in drinking water treatment plants known as Drinking Water Treatment Sludge (DWTS) is continuously increasing all around the world. Currently, DWTS is disposed to sanitary sewers, streams, and landfills. Land application is another solution for the management of DWTS [1]. It contains coagulants, heavy metals, clays, and organic matters. Some metals in the sludge can accumulate into exposed environment and may cause significant risk to living organisms and the human [1,2]. From the economic and environmental aspects, the recycling of DWTS has become more attractive and vital option [2]. Some of the main recycling options are: cement, brick, and ceramic production, sewage sludge dewatering, agricultural practices, removal of contaminants from wastewater, and wetland. Recently, recovery of coagulants (iron and aluminum salts) from sludge by acid or alkali treatments have been extensively considered [1–6]. The obtained material can be utilized as adsorbent, carrier, and chemical precursors. For instance, Meng et al. [2] recovered Fe<sup>3+</sup> from DWTS and synthesized iron oxide-SiO<sub>2</sub> composite for reactive dye and NaNO<sub>2</sub>

adsorption.

Nano scale iron particles are recently receiving extensive attention due to their special properties. Over the last few years, various physical, chemical, and biological methods (e.g. co-precipitation, hydrothermal, sonochemical, and hydrolysis) have been employed to synthesize iron nanoparticles (NPs) [7–10]. Green synthesis however, is a clean, biocompatible, non-toxic, cost-effective and eco-friendly method for synthesis of NPs [11–13]. Green synthesis of iron NPs using different plant extracts such as eucalyptus leaf [14,15], Mangifera indica, Magnolia champaca, Azadirachta indica, and Murraya koenigii leaf [16,17], green and black tea leaf [18–20], microorganisms [21,22], and alga extract [23] have been reported.

Since iron is an essential nutrient for all organisms, iron NPs have been considered as a potential micronutrient for methanogenesis bacteria in anaerobic digestion (AD) of organic wastes [24] which are suitable sources for retrieving energy [25]. In biogas production, supply of micro-nutrient supplements not only stimulate the methane production, but also improve the process stability [26–30]. Among various additives, iron NPs are proven to improve methane yield, decline aromas (e.g. H<sub>2</sub>S) and facilitate the removal of chemical oxygen demand (COD) during the AD [31]. Recently, Suanon et al. [31] investigated the influence of iron NPs on methane production during the AD of sewage sludge.

\* Corresponding author.

E-mail address: [heidari@ferdowsi.um.ac.ir](mailto:heidari@ferdowsi.um.ac.ir) (A. Heidari).

In all the aforementioned studies, commercial chemical precursors with analytical grades (e.g.  $\text{FeSO}_4$ ,  $\text{FeNO}_3$  and  $\text{FeCl}_2$ ) had been used for biosynthesis of iron NPs. Therefore, the present paper is the first report on successful biosynthesis of iron NPs from DWTS. Moreover, not any effort has been done on assessing the effect of biosynthesized iron NPs on the performance of AD of slaughterhouse wastewater (SW). Hence, the possibility of improving biogas yield from AD of SW using the biosynthesized NPs was investigated.

## 2. Materials and method

### 2.1. Iron recovery and biosynthesis

#### 2.1.1. Materials

The DWTS used in this survey was collected from a water treatment plant (number 1) in Mashhad, Iran. The plant utilizes ferric chloride as coagulant and calcium carbonate for pH adjustment. In the laboratory, the DWTS sample was air dried at  $70^\circ\text{C}$  for two days. Then the dried sludge was crushed and sieved. Chemical composition of DWTS was determined using X-ray fluorescence spectrometry (PW1404, Philips spectrometer). HCl and NaOH were purchased from Merck Co (Merck, Germany). For the biosynthesis test, black tea was obtained from Lahijan tea cultivation farms in Guilan province, Iran.

#### 2.1.2. Iron recovery

Iron recovery was conducted according to the method reported by Meng et al. [32]. HCl (2 M) was applied to wash out the mineral ingredients from the DWTS. 15 g of DWTS was acid-washed by a liquid/solid (L/S) ratio of 20:1 at  $90^\circ\text{C}$  for 3 h under constant stirring. After the acid treatment, the mixture was filtered and the obtained solution was used for the biosynthesis of iron nanoparticles and further analysis. The color of this solution was yellow. The filtrates were characterized by ICP-OES analyzer. Fe ( $8723\text{ mg L}^{-1}$ ), Ca ( $2706\text{ mg L}^{-1}$ ), Mg ( $550\text{ mg L}^{-1}$ ), Al ( $448\text{ mg L}^{-1}$ ), and Si ( $49\text{ mg L}^{-1}$ ) were found in the sample.

#### 2.1.3. Biosynthesis of iron NPs

For the biosynthesis of iron NPs, the plant extract was firstly prepared by adding 20 g of black tea in 1 L distilled water at  $80^\circ\text{C}$  for 1 h. Then, a certain amount of extract was added to iron recovery solution with the ratio of 4:1 (by volume) with constant stirring until the color of the solution mixture was turned yellow to black. After that, the obtained product was centrifuged at 12000 rpm and then washed with distilled water and methanol for several times. Finally, the synthesized iron NPs were dried at room temperature.

#### 2.1.4. Characterization of the synthesized iron NPs

The synthesized iron NPs were characterized using UV–visible spectrophotometer (DR 5000, HACH, USA) from 200 to 800 nm. The X ray diffraction (XRD) analysis was performed using an X-ray diffractometer (PW1730, Philips, Italy) in the scanning range ( $2\theta$ ) of  $10$ – $90^\circ$ . The instrument worked at a voltage of 40 kV and a current of 30 mA with monochromatic Cu  $K\alpha$  radiation. Fourier-transform infrared spectroscopy (FT-IR) (AVATAR 370, Thermo Nicolet, USA) was applied to specify the different functional groups on iron NPs. Field emission scanning electron microscopy (FESEM) images were provided by an electron microscope (MIRA3, TE-SCAN, Czech Republic). Elemental compositions of the DWTS was identified by an X-ray Fluorescence Spectrometer (Philips PW 1480, Netherlands).

### 2.2. AD of SW

#### 2.2.1. Substrate and inoculum

SW samples were taken from a slaughterhouse located in Mashhad, Iran. It is one of the biggest plant of this kind in Iran, with an hourly throughput of up to 300 sheep. The samples were quickly transferred to the biogas laboratory at Ferdowsi University of Mashhad (FUM) and was stored at  $4^\circ\text{C}$ . Digestate from a biogas pilot plant fed with dairy manure located at the laboratory was used as inoculum. The inoculum was stored under mesophilic condition for further degradation and biogas removal. The characteristics of SW is listed in Table 1.

#### 2.2.2. Batch AD experiments

The batch tests were conducted in bottles of 250 mL, connecting to a 1000 mL gas collecting bag. The bottles were loaded with inoculum to substrate ratio (ISR) of about 3.5 (VS-basis) to prevent acidification as suggested by Ref. [33] (50 mL of inoculum and 150 mL of SW). The initial pH, TS and COD of the mixture were 7, 1.95%, and  $9835\text{ mg L}^{-1}$ , respectively. The synthesized Fe NPs was added to the digesters in three different concentrations (3, 9, and  $15\text{ mg L}^{-1}$ ). A reactor without Fe NPs was also prepared as control reactor. Moreover, three blank assays were run with inoculum only to determine its remaining biogas and methane yield. This yield was subtracted from those obtained from other reactors. All the tests were performed in triplicate. The headspace was purged with nitrogen gas for 45 s to perform anaerobic condition [34]. The initial pH of the mixture in all the reactors was in neutral range, hence there was no need to add alkaline for pH adjustment. The temperature of the bottles was maintained constant at  $35^\circ\text{C}$  in a thermostatic water bath.

#### 2.2.3. Analytical procedures

Substrate and inoculum characteristics such as, TS, VS and COD were determined according to the standard methods [35]. The pH of the materials was measured with an Ion Concentration/pH meter (DR359Tx, EDT Direction Ltd, UK). The reactors were shaken once a day for about 30 s before biogas sampling. The volume of the biogas collected in the collecting bag was measured by a syringe on a daily basis. The methane concentration was measured by Einhorn's Fermentation-Saccharometer as described in Refs. [36,37].

## 3. Results and discussion

### 3.1. DWTS characterization

The chemical composition of the DWTS was presented in Table 2. As can be seen in Table 2, there were various metal and non-metal oxides in the DWTS. Among these,  $\text{Fe}_2\text{O}_3$  (33.3%),  $\text{SiO}_2$  (20.4%), CaO (8.1%) and  $\text{Al}_2\text{O}_3$  (6.1%) were the main components of the DWTS. The amount of other oxides such as  $\text{K}_2\text{O}$ ,  $\text{Na}_2\text{O}$ ,  $\text{TiO}_2$ , MnO,  $\text{P}_2\text{O}_5$ , and  $\text{SO}_3$  were less than 2%. The presence of  $\text{Fe}_2\text{O}_3$  in the sludge structure are related to the use of ferric chloride as coagulant in drinking water treatment where they are used to settle down the suspended solids like clay and sand from water. Beside,  $\text{SiO}_2$  in the DWTS is originated from clay minerals and free silica particles. XRD analysis confirmed the presence of these metal compounds as shown in Fig. 1. Some trace metals also found in the sludge. Zn, Cl, and Ba have the highest concentration in DWTS, respectively.

### 3.2. Characterization of iron NPs

#### 3.2.1. UV–visible

The formation of the iron NPs using black tea extract was monitored visually and by UV–visible spectroscopy and displayed

**Table 1**  
The characteristics of slaughterhouse wastewater.

Parameter	COD mg.L <sup>-1</sup>	BOD <sub>5</sub> mg.L <sup>-1</sup>	TS <sup>a</sup>	VS (%)	C (% of TS)	N (% of TS)	H (% of TS)	S (% of TS)	C/N
	4462	3123	0.6	0.31	27.3	2.6	4.2	1.78	10.3

<sup>a</sup> Percent of fresh feedstock.

**Table 2**  
Chemical composition of dried DWTS.

Components	Quantity (wt. %)	Elements	Quantity (ppm)
Fe <sub>2</sub> O <sub>3</sub>	33.33	Zn	1772
SiO <sub>2</sub>	20.40	Cl	1214
CaO	8.18	Ba	704
Al <sub>2</sub> O <sub>3</sub>	6.19	Sr	282
K <sub>2</sub> O	2.11	V	115
MgO	1.83	Cr	108
MnO	0.88	Co	92
TiO <sub>2</sub>	0.40	Rb	72
SO <sub>3</sub>	0.38	Ni	69
Na <sub>2</sub> O	0.33	Mo	26
P <sub>2</sub> O <sub>5</sub>	0.31	Y	17
LOI	25.04	Nb	14

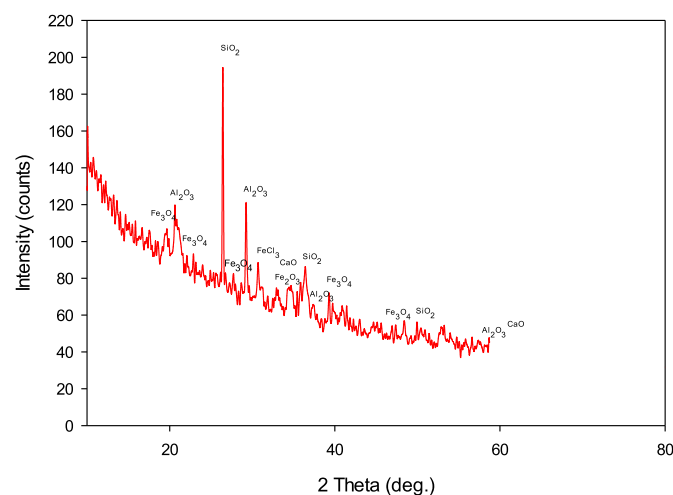


**Fig. 1.** XRD pattern of DWTS.

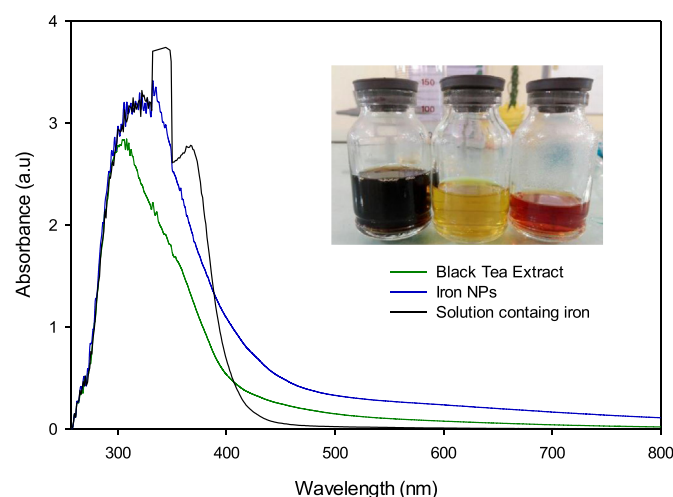


**Fig. 2.** UV-visible spectra of black tea extract, iron NPs, and acid washing solution containing iron.

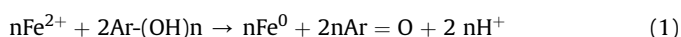
in Fig. 2. After adding the tea extract into iron aqueous solution, the color of the reaction mixture changed immediately from yellow to black, indicating the creation of iron NPs. Furthermore, as can be seen in Fig. 2, in UV-visible spectrums, the control sample showed a distinct peak at 344 nm. The absorption peak at 308 nm correlated to the tea polyphenols and caffeine of tea extract. After the reduction process, the peak shifted to a broad continuous adsorption band (Fig. 2). It proves that the polyphenols and caffeine in tea extract acted as reducing agents and convert iron into iron NPs. These results are in consistent with prior studies on biosynthesis of iron NPs using black and green tea extract [16,18,38].

### 3.2.2. FESEM and EDX analysis

Fig. 3 shows the FESEM images of iron NPs synthesized using black tea leaf extract. It can be seen that the obtained iron NPs have spherical shape with diameter in the range 20–30 nm. Similar results have been reported for iron NPs prepared by different tea extracts [11,14,18]. Moreover, the iron NPs tended to aggregate probably due to the existence of polyphenols or antioxidants in the tea extract acting as the reducing and capping agents, which can deduct the aggregation of iron NPs compared to chemically synthesized materials [15]. The elemental composition of the synthesized iron NPs was determined by the EDX. In the EDX spectrum, three intense peaks of C, O and Fe was found, which verified the formation of iron NPs by black tea extract. The C and O signals arose from the polyphenol groups and other C, O-containing molecules in the tea extract [14]. The weight percentages of C, O and Fe in the obtained product were 60.18%, 18.78%, and 11.04%, respectively. These results are in consistent with Lin et al. study [39].

### 3.2.3. FT-IR analysis

FTIR spectra of the iron NPs displays some peaks in the spectral span 400–4000 cm<sup>-1</sup> (Fig. 4). The very strong peak at 3409 cm<sup>-1</sup> relates to the stretching vibration of O–H of phenolic compound [16,39], and of around 2917 cm<sup>-1</sup> is ascribed to the asymmetric C–H and CH<sub>2</sub> vibrations of aliphatic hydrocarbons [16,40]. Moreover, the peak around 1626 cm<sup>-1</sup> can be attributed to the C=O ring stretching in polyphenols [39,41]. Eventually, two peaks around 530 and 447 cm<sup>-1</sup> refer to Fe–O stretches of Fe<sub>2</sub>O<sub>3</sub> and Fe<sub>3</sub>O<sub>4</sub> [14,16,39], that confirm properly the synthesis of Fe NPs. The formation of iron NPs can be explained with polyphenolic compounds which present in black tea extract [15,42]. In fact, the phenyl groups (Ar) directly reduced the iron ions to iron zero-valent particles as follow [14,15,43]:



### 3.2.4. XRD analysis

The crystal structure of as prepared iron NPs was determined by XRD. As displayed in Fig. 5, there is no distinctive diffraction peaks in XRD pattern, indicating that obtained sample is amorphous in nature. The distinctive peak at  $2\theta = 21.45$  is related to the organic materials polyphenols/caffeine) of tea extract which adsorbed on NPs [44,45]. Furthermore, small intensity peak appearing at  $2\theta = 44.9$  ascribed to zero-valent iron (a-Fe). Similar reflections

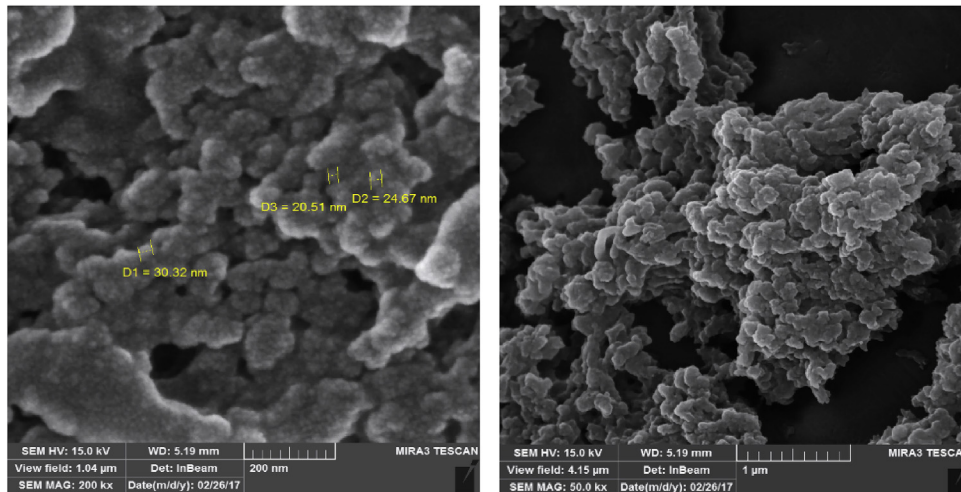


Fig. 3. SEM images of iron NPs.

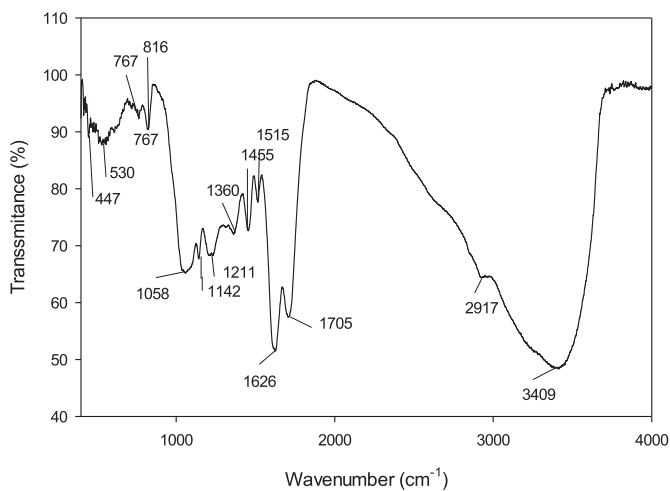


Fig. 4. FTIR spectra of iron NPs.

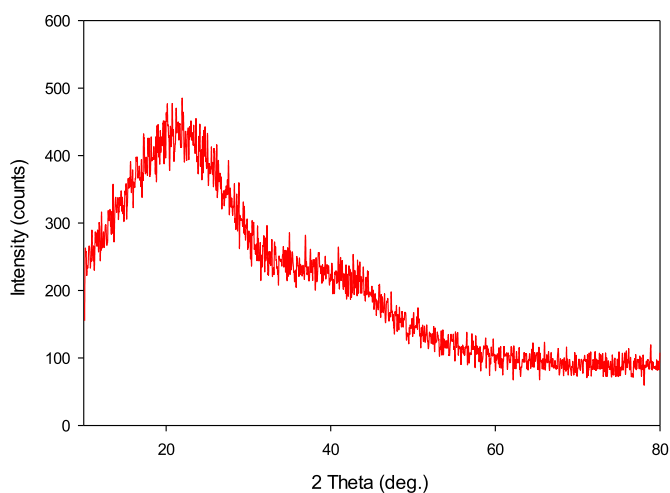


Fig. 5. XRD pattern of iron NPs.

were seen in XRD pattern of iron NPs biosynthesized by green tea [45], black tea [18], sorghum bran [46], and Terminalia chebula [41].

### 3.3. The effect of synthesized NPs on AD of SW

#### 3.3.1. Biogas yield

High content of COD and BOD of SW (Table 1) makes it an interesting feedstock for AD to produce energy in the form of methane. The effect of different concentrations of the bio-synthesized iron NPs in AD of SW was shown in Fig. 6.

As can be seen in the figure, addition of iron NPs in all concentrations enhanced the startup of biogas production and shortened the lag phase. The lag phase for control digester lasted 5 days during which, only  $64 \text{ NL kg}^{-1} \text{ VS}$  of biogas (with 12%  $\text{CH}_4$ ) was produced. The maximum biogas yield during this period was obtained from the reactor with  $9 \text{ mg L}^{-1}$  additive ( $202.46 \text{ NL kg}^{-1} \text{ VS}$ ) ( $P < 0.05$ ), whereas the yield from reactors with 3 and  $15 \text{ mg/L}$  additive was  $174.58$  and  $156.66 \text{ NL kg}^{-1} \text{ VS}$ , respectively. Biogas production dropped in 7th day and no biogas was produced until day 14th for all the digesters, presenting a severe inhibition. Since this occurred in all the digesters including the control, the inhibition could be due to the inherent characteristics of the SW. Over production and accumulation of volatile fatty acids (VFA) that inhibited the methanogens activities could be the reason [47]. After 7 days of self-recovery, biogas production started again by following an almost similar curve slope in all the digesters. While a biogas yield of  $610 \text{ NL kg}^{-1} \text{ VS}$  was achieved from control digester, the highest biogas yield was obtained from 3 to  $9 \text{ mg L}^{-1}$  of additives. This corresponds to up to 37.6% enhancement over the control reactor. Nevertheless, more dosage of additive led to lower production ( $P < 0.01$ ). Inhibition effect of an element depends on its concentration, substrate, and the adaptation of the microorganisms to that element. This concentration is usually very low [48]. Therefore, excess concentration of iron NPs would be toxic [49]. The minimum concentration of iron NPs as trace element should be between 1 and  $10 \text{ mg L}^{-1}$  [50] which was considered in this study.

The methane yield is a key index to evaluate the AD performance. Similar to the biogas yield, addition of 3 and  $9 \text{ mg L}^{-1}$  iron NPs significantly increased the methane yield (up to 44%) over the control ( $P < 0.01$ ). The methane content for reactors treated by 3, 9,  $15 \text{ mg L}^{-1}$  of DWTS was 71.89, 71.99, and 74.54 respectively, while it

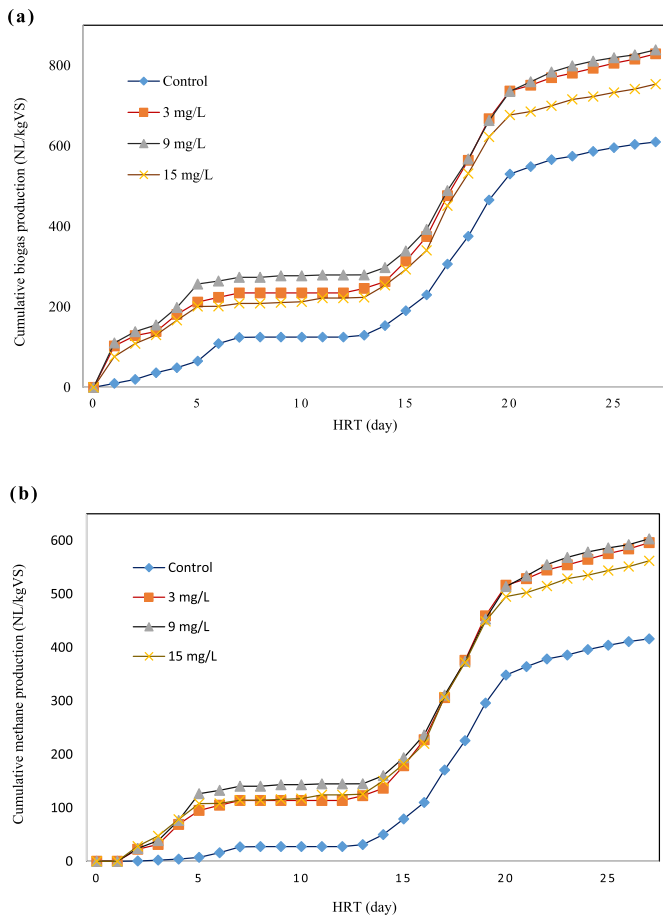
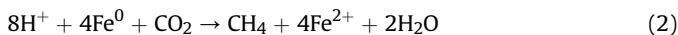


Fig. 6. The effect of different dosage of iron NPs on cumulative (a) biogas and (b) methane production.

Table 3  
Effect of iron NPs on AD of different feed stocks in mesophilic condition.

Feedstock	Iron type	Optimum concentration (mg.L <sup>-1</sup> )	Enhanced Methane yield (%)	Ref.
Sewage sludge	Nano iron	1000	25.1	[31]
Cow manure	Fe <sub>3</sub> O <sub>4</sub> NPs	16.67	45	[51]
Sewage sludge	NZVI	–	40.4	[29]
Manure	Fe <sub>3</sub> O <sub>4</sub> NPs	20	95	[27]
SW	Fe NPs	9	45	Present work

was 68.20 for control. These enhancements in the methane yield can be related to the partial conversion of produced CO<sub>2</sub> to methane in the presence of iron NPs via the electron transmission [31] as presented in equation (2).



### 3.3.2. pH and COD

The pH value is an important factor affecting the digestion process. The value of pH at the end of the runs for the reactors with 0, 3, 9 and 15 mg L<sup>-1</sup> additive was 7.70, 7.35, 7.37 and 7.32, respectively. Having pH in the neutral range not only shows the favorable conditions during the AD, but also confirms the stability of the digestion. Furthermore, the impact of iron NPs on COD

reduction was investigated. The COD reduction in control reactor was 51% while it improved to 72% for 3 and 9 mg L<sup>-1</sup>, and 70% for 15 mg L<sup>-1</sup> of iron NPs. It can easily be understood that iron NPs had positive impact on COD reduction. The COD removal efficiency enhancement of 38–42% over the control digester was obtained by the use of iron NPs. These results are very interesting from the practical point of view. In large scale biogas plants, application of NPs would be very costly while, recovery of these materials from sludge could be more economic and environmentally friendly way. However, further researches are needed for scale up and process optimization.

The results from the use of iron NPs in the AD of SW were compared with literature (see Table 3). The improvement in methane yield through the addition of different types of iron varies from 9% up to 95%. For example, Suanon et al. [31] studied the application of nano scale iron and iron powder during sludge anaerobic digestion. Their results demonstrated 25% increase in the methane yield [31]. Moreover, Abdelsalam et al. [27] reported an increase of 95% methane from anaerobic digestion of manure using different iron NPs. In the present study, an enhancement up to 45% in methane yield was achieved from the AD of SW. It is worthy to be mentioned that in these literature, the NPs were purchased from credible companies with high purity, or were prepared with chemical synthesis methods from the laboratory materials. Nonetheless, the results from the present work is comparable with those obtained using high purity NPs.

## 4. Conclusion

Iron NPs from DWTS was successfully biosynthesized using black tea extract and was confirmed by UV–visible spectroscopy, XRD, SEM, EDX, and FTIR analyses. The synthesized NPs were sphere-like with diameter in the range of 20–40 nm. This product was used as micronutrients in AD of SW. The results indicated that adding different concentrations of iron NPs into the digester, leads

to increase in methane production up to 45%. Furthermore, it significantly improved the COD reduction.

## Acknowledgments

This research was financially supported by Ferdowsi University of Mashhad (FUM), Mashhad, Iran (Research ID 43452). The authors would also like to appreciate kindly help of the Agricultural Machinery Research Center of FUM.

## References

- [1] T. Ahmad, K. Ahmad, M. Alam, Sustainable management of water treatment sludge through 3'R' concept, *J. Clean. Prod.* 124 (2016) 1–13.
- [2] L. Meng, Y. Chan, H. Wang, Y. Dai, X. Wang, J. Zou, Recycling of iron and silicon from drinking water treatment sludge for synthesis of magnetic iron oxide@SiO<sub>2</sub> composites, *Environ. Sci. Pollut. Control Ser.* 23 (2016) 5122–5133.

- [3] D.Y.Y. Tay, R. Fujinuma, L.A. Wendling, Drinking water treatment residual use in urban soils: balancing metal immobilization and phosphorus availability, *Geoderma* 305 (2017) 113–121.
- [4] H. Xu, M. Ding, K. Shen, J. Cui, W. Chen, Removal of aluminum from drinking water treatment sludge using vacuum electrokinetic technology, *Chemosphere* 173 (2017) 404–410.
- [5] C. Wang, N. Yuan, Y. Pei, H.-L. Jiang, Aging of aluminum/iron-based drinking water treatment residuals in lake water and their association with phosphorus immobilization capability, *J. Environ. Manag.* 159 (2015) 178–185.
- [6] A.T. Nair, M.M. Ahammed, Influence of sludge characteristics on coagulant recovery from water treatment sludge: a preliminary study, *J. Mater. Cycles Waste Manag.* 19 (2017) 1228–1234.
- [7] S.-Y. Yoon, C.-G. Lee, J.-A. Park, J.-H. Kim, S.-B. Kim, S.-H. Lee, J.-W. Choi, Kinetic, equilibrium and thermodynamic studies for phosphate adsorption to magnetic iron oxide nanoparticles, *Chem. Eng. J.* 236 (2014) 341–347.
- [8] S. Giri, S. Samanta, S. Maji, S. Ganguli, A. Bhaumik, Magnetic properties of  $\alpha$ -Fe<sub>2</sub>O<sub>3</sub> nanoparticle synthesized by a new hydrothermal method, *J. Magn. Magn. Mater.* 285 (2005) 296–302.
- [9] C.H.Y. Shik Chi Tsang, Xin Gao, Kin tam silica-encapsulated nanomagnetic particle as a new recoverable biocatalyst Carrier, *J. Phys. Chem. B* 110 (2006) 16914–16922.
- [10] A. Hassanjani-Roshan, M.R. Vaezi, A. Shokuhfar, Z. Rajabali, Synthesis of iron oxide nanoparticles via sonochemical method and their characterization, *Particuology* 9 (2011) 95–99.
- [11] L. Huang, F. Luo, Z. Chen, M. Megharaj, R. Naidu, Green synthesized conditions impacting on the reactivity of Fe NPs for the degradation of malachite green, *Spectrochim. Acta Mol. Biomol. Spectrosc.* 137 (2015) 154–159.
- [12] M. Sajjadi, M. Nasrollahzadeh, S. Mohammad Sajadi, Green synthesis of Ag/Fe<sub>3</sub>O<sub>4</sub> nanocomposite using *Euphorbia peplus* Linn leaf extract and evaluation of its catalytic activity, *J. Colloid Interface Sci.* 497 (2017) 1–13.
- [13] G. Sharmila, M. Farzana Fathima, S. Haries, S. Geetha, N. Manoj Kumar, C. Muthukumar, Green synthesis, characterization and antibacterial efficacy of palladium nanoparticles synthesized using *Filicium decipiens* leaf extract, *J. Mol. Struct.* 1138 (2017) 35–40.
- [14] T. Wang, J. Lin, Z. Chen, M. Megharaj, R. Naidu, Green synthesized iron nanoparticles by green tea and eucalyptus leaves extracts used for removal of nitrate in aqueous solution, *J. Clean. Prod.* 83 (2014) 413–419.
- [15] T. Wang, X. Jin, Z. Chen, M. Megharaj, R. Naidu, Green synthesis of Fe nanoparticles using eucalyptus leaf extracts for treatment of eutrophic wastewater, *Sci. Total Environ.* 466–467 (2014) 210–213.
- [16] C.P. Devatha, A.K. Thalla, S.Y. Katte, Green synthesis of iron nanoparticles using different leaf extracts for treatment of domestic waste water, *J. Clean. Prod.* 139 (2016) 1425–1435.
- [17] S. Machado, S.L. Pinto, J.P. Grosso, H.P.A. Nouws, J.T. Albergaria, C. Delerue-Matos, Green production of zero-valent iron nanoparticles using tree leaf extracts, *Sci. Total Environ.* 445–446 (2013) 1–8.
- [18] L. Huang, X. Weng, Z. Chen, M. Megharaj, R. Naidu, Green synthesis of iron nanoparticles by various tea extracts: comparative study of the reactivity, *Spectrochim. Acta Mol. Biomol. Spectrosc.* 130 (2014) 295–301.
- [19] V. Smuleac, R. Varma, S. Sikdar, D. Bhattacharyya, Green synthesis of Fe and Fe/Pd bimetallic nanoparticles in membranes for reductive degradation of chlorinated organics, *J. Membr. Sci.* 379 (2011) 131–137.
- [20] S. Machado, W. Stawiński, P. Slonina, A.R. Pinto, J.P. Grosso, H.P.A. Nouws, J.T. Albergaria, C. Delerue-Matos, Application of green zero-valent iron nanoparticles to the remediation of soils contaminated with ibuprofen, *Sci. Total Environ.* 461–462 (2013) 323–329.
- [21] A.A. Bharde, R.Y. Parikh, M. Baidakova, S. Jouen, B. Hannoyer, T. Enoki, B.L.V. Prasad, Y.S. Shouche, S. Ogale, M. Sastry, Bacteria-mediated precursor-dependent biosynthesis of superparamagnetic iron oxide and iron sulfide nanoparticles, *Langmuir* 24 (2008) 5787–5794.
- [22] J.-W. Moon, C.J. Rawn, A.J. Rondinone, L.J. Love, Y. Roh, S.M. Everett, R.J. Lauf, T.J. Phelps, Large-scale production of magnetic nanoparticles using bacterial fermentation, *J. Ind. Microbiol. Biotechnol.* 37 (2010) 1023–1031.
- [23] M. Mahdavi, F. Namvar, M. Ahmad, R. Mohamad, Green biosynthesis and characterization of magnetic iron oxide (Fe<sub>3</sub>O<sub>4</sub>) nanoparticles using seaweed (*Sargassum muticum*) aqueous extract, *Molecules* 18 (2013) 5954.
- [24] Y.Y. Choong, I. Norli, A.Z. Abdullah, M.F. Yhaya, Impacts of trace element supplementation on the performance of anaerobic digestion process: a critical review, *Bioresour. Technol.* 209 (2016) 369–379.
- [25] R. Rathaur, S.H. Dhawane, A. Ganguly, M.K. Mandal, G. Halder, Methanogenesis of organic wastes and their blend in batch anaerobic digester: experimental and kinetic study, *Process Saf. Environ. Protect.* 113 (2018) 413–423.
- [26] M.S. Romero-Güiza, J. Vila, J. Mata-Alvarez, J.M. Chimenos, S. Astals, The role of additives on anaerobic digestion: a review, *Renew. Sustain. Energy Rev.* 58 (2016) 1486–1499.
- [27] E. Abdelsalam, M. Samer, Y.A. Attia, M.A. Abdel-Hadi, H.E. Hassan, Y. Badr, Influence of zero valent iron nanoparticles and magnetic iron oxide nanoparticles on biogas and methane production from anaerobic digestion of manure, *Energy* 120 (2017) 842–853.
- [28] E. Abdelsalam, M. Samer, Y.A. Attia, M.A. Abdel-Hadi, H.E. Hassan, Y. Badr, Effects of Co and Ni nanoparticles on biogas and methane production from anaerobic digestion of slurry, *Energy Convers. Manag.* 141 (2017) 108–119.
- [29] L. Su, X. Shi, G. Guo, A. Zhao, Y. Zhao, Stabilization of sewage sludge in the presence of nanoscale zero-valent iron (nZVI): abatement of odor and improvement of biogas production, *J. Mater. Cycles Waste Manag.* 15 (2013) 461–468.
- [30] J. Pessuto, B.S. Scopel, D. Perondi, M. Godinho, A. Dettmer, Enhancement of biogas and methane production by anaerobic digestion of swine manure with addition of microorganisms isolated from sewage sludge, *Process Saf. Environ. Protect.* 104 (2016) 233–239.
- [31] F. Suanon, Q. Sun, M. Li, X. Cai, Y. Zhang, Y. Yan, C.-P. Yu, Application of nanoscale zero valent iron and iron powder during sludge anaerobic digestion: impact on methane yield and pharmaceutical and personal care products degradation, *J. Hazard Mater.* 321 (2017) 47–53.
- [32] L. Meng, Y. Chan, H. Wang, Y. Dai, X. Wang, J. Zou, Recycling of iron and silicon from drinking water treatment sludge for synthesis of magnetic iron oxide/SiO<sub>2</sub> composites, *Environ. Sci. Pollut. Control Ser.* 23 (2016) 5122–5133.
- [33] C. Holliger, M. Alves, D. Andrade, I. Angelidaki, S. Astals, U. Baier, C. Bougrier, P. Buffière, M. Carballa, V. de Wilde, Towards a standardization of biomethane potential tests, *Water Sci. Technol.* 74 (2016) 2515–2522.
- [34] T. Forster-Carneiro, M. Pérez, L. Romero, Thermophilic anaerobic digestion of source-sorted organic fraction of municipal solid waste, *Bioresour. Technol.* 99 (2008) 6763–6770.
- [35] A.P.H. Association, A.W.W. Association, W.P.C. Federation, W.E. Federation, Standard Methods for the Examination of Water and Wastewater, American Public Health Association, 1915.
- [36] L. Kaluža, M. Sušarskić, V. Rutar, G.D. Zupančič, The re-use of Waste-Activated Sludge as part of a “zero-sludge” strategy for wastewater treatments in the pulp and paper industry, *Bioresour. Technol.* 151 (2014) 137–143.
- [37] M. Ahmadi-Pirlou, M. Ebrahimi-Nik, M. Khojastehpour, S.H. Ebrahimi, Mesophilic co-digestion of municipal solid waste and sewage sludge: effect of mixing ratio, total solids, and alkaline pretreatment, *Int. Biodeterior. Biodegrad.* 125 (2017) 97–104.
- [38] M.N. Nadagouda, A.B. Castle, R.C. Murdock, S.M. Hussain, R.S. Varma, In vitro biocompatibility of nanoscale zerovalent iron particles (NZVI) synthesized using tea polyphenols, *Green Chem.* 12 (2010) 114–122.
- [39] J. Lin, X. Weng, R. Dharmarajan, Z. Chen, Characterization and reactivity of iron based nanoparticles synthesized by tea extracts under various atmospheres, *Chemosphere* 169 (2017) 413–417.
- [40] T. Shahwan, S. Abu Sirriah, M. Nairat, E. Boyacı, A.E. Eroğlu, T.B. Scott, K.R. Hallam, Green synthesis of iron nanoparticles and their application as a Fenton-like catalyst for the degradation of aqueous cationic and anionic dyes, *Chem. Eng. J.* 172 (2011) 258–266.
- [41] K. Mohan Kumar, B.K. Mandal, K. Siva Kumar, P. Sreedhara Reddy, B. Sreedhar, Biobased green method to synthesise palladium and iron nanoparticles using *Terminalia chebula* aqueous extract, *Spectrochim. Acta Mol. Biomol. Spectrosc.* 102 (2013) 128–133.
- [42] J.M. Lorenzo, P.E.S. Munekata, Phenolic compounds of green tea: health benefits and technological application in food, *Asian Pacific Journal of Tropical Biomedicine* 6 (2016) 709–719.
- [43] S.A.O. Santos, J.J. Villaverde, C.S.R. Freire, M.R.M. Domingues, C.P. Neto, A.J.D. Silvestre, Phenolic composition and antioxidant activity of *Eucalyptus grandis*, *E. urograndis* (*E. grandis* × *E. urophylla*) and *E. maidenii* bark extracts, *Ind. Crop. Prod.* 39 (2012) 120–127.
- [44] M. Colon, C. Nerin, Role of catechins in the antioxidant capacity of an active film containing green tea, green coffee, and grapefruit extracts, *J. Agric. Food Chem.* 60 (2012) 9842–9849.
- [45] G.E. Hoag, J.B. Collins, J.L. Holcomb, J.R. Hoag, M.N. Nadagouda, R.S. Varma, Degradation of bromothymol blue by ‘greener’ nano-scale zero-valent iron synthesized using tea polyphenols, *J. Mater. Chem.* 19 (2009) 8671–8677.
- [46] E.C. Njagi, H. Huang, L. Stafford, H. Genuino, H.M. Galindo, J.B. Collins, G.E. Hoag, S.L. Suib, Biosynthesis of iron and silver nanoparticles at room temperature using aqueous sorghum bran extracts, *Langmuir* 27 (2011) 264–271.
- [47] D. Brown, Y. Li, Solid state anaerobic co-digestion of yard waste and food waste for biogas production, *Bioresour. Technol.* 127 (2013) 275–280.
- [48] D. Deublein, A. Steinhäuser, Substrate. Biogas from Waste and Renewable Resources, Wiley-VCH Verlag GmbH & Co. KGaA, 2010, pp. 55–84.
- [49] M.A. Ganzoury, N.K. Allam, Impact of nanotechnology on biogas production: a mini-review, *Renew. Sustain. Energy Rev.* 50 (2015) 1392–1404.
- [50] D. Deublein, A. Steinhäuser, Biogas from Waste and Renewable Resources: an Introduction, John Wiley & Sons, 2011.
- [51] S. Juntupally, S. Begum, S.K. Allu, S. Nakkasunchi, M. Madugula, G.R. Anupoju, Relative Evaluation of Micronutrients (Mn) and its Respective Nanoparticles (Nps) as Additives for the Enhanced Methane Generation, *Bioresour. Technol.*